Supporting Information for the manuscript

A Luminescent Nanoscale Metal-Organic Framework with Controllable Morphologies for Spore Detection

Hui Xu,[a] Xingtang Rao,[a] Junkuo Gao,[a] Jiancan Yu,[a] Ziqi Wang,[a] Zhongshang Dou,[a] Yuanjing Cui,[a] Yu Yang,[a] Banglin Chen*[ab] and Guodong Qian*[a]

[a] State Key Laboratory of Silicon Materials, Department of Materials Science & Engineering, Zhejiang University, Hangzhou, 310027 P. R. China, [b] Department of Chemistry, University of Texas at San Antonio, San Antonio, TX 78249-0698 , USA

*Corresponding Authors. E-mail: gdqian@zju.edu.cn, banglin.chen@utsa.edu

Experimental Section

The methylammonium salt of fumaric acid and oxalate acid were synthesized by dissolving fumaric acid (0.01mol, 1.16g) and oxalate acid (0.00167mol, 0.15g) in methylamine(10ml, 40wt% in water) and dried under reduced pressure. Then the salt was dissolved in distilled water to form a solution with 0.3M fumaric and 0.05M oxalate salt.

The nanoscale **NMOF 1** was synthesized through the microemulsion method at elevated temperature, 150 ℃ for 48h. For a typical synthesis with W=20: Firstly, two microemulsion systems contain cetyltrimethylammonium bromide(CTAB)(0.91g, 2.5mmol),1-hexanol(3.13ml, 0.025mol) and iso-octane(45.87ml, 0.2771mol) were stirred respectively for 30min. Two aqueous solutions of $Eu(NO_3)_3{\cdot}6H_2O$(0.90ml,

0.1M) and the methylammoium salt of fumaric and oxalate salts(0.90ml, 0.3M for fumaric salt and 0.05M for oxalate salt) were added to the microemulsion systems respectively, after stirred for 30 min, the microemulsions termed to be transparent. Then the two microemulsions were mixed together and stirred vigorously for at least another 30 min at room temperature. Then the microemulsion system was transferred to Teflon-lined parr reactor, and the reaction mixture were then heated at 150 ℃ for 48 h. The obtained solution was centrifugated at 3000 rpm for 5 min to give the elongated hexagonal nanoplates. The elongated hexagonal nanoplates were washed and redispersed in ethanol by sonificated for 5min and centrifugated again by the same method. This centrifugation and redispersement was repeated for twice and finally give the ethanol solution of **NMOF 1**. The PXRD sample was prepared by drying the ethanol solution of **NMOF 1** under 60 ℃ overnight. TGA showed that there is a continuing weight loss in the range of 120-280℃, as indicated in Figure S1, the total weight loss is 17.94%, in agreement with the calculated value of 18.9% for the total 8 water molecules per formula. And 34.29% in the range of 380-800 ℃ is attributed to the decomposition of the dehydrated phase. The final residues 46.67% is in agreement with the calculated value of 46.0% based on Eu_2O_3. Elemental analysis: Anal. Calcd for $C_{10}H_{20}O_{20}Eu_2$: C, 15.72; H, 2.64. Found: C, 15.39; H, 2.39.
The sensing experiments of the **NMOF 1** was performed by adding 20μl aqueous solutions of different concentration of DPA and other analytes to 2ml **NMOF 1** ethanol solution and measured the PL spectra. For the sensing experiments of the bulk **MOF 1**, 50mg bulk crystal powder was immersed in 2ml different concentration of DPA ethanol solution for several minutes, and dried in 60℃ and measured the PL spectra.

Computer Morphology Simulation

Morphology predictions were performed using the Morphology tool implemented in Materials Studio version 4.3. Crystal structures used to simulate morphology were

determined from single crystal X-ray diffraction data. The **MOF 1** crystallographic information files (CIF) are obtained from the CCDC. A list of growth facets is generated according to the Bravais-Friedel-Donnary-Harker rules. The minimum interplanar spacing for face list generation was set to 1.3 Å, and the maximum absolute value for the Miller indices h, k and l for the faces were set to 4, 4, and 4, respectively, with an upper limit of 200 growing faces. After face generation, BFDH method is applied for morphology simulation under different facets growth rates conditions.

Instrumental Analysis

Powder XRD diffractograms were measured by RIGAMU D/MAX 2550/PC X-ray diffractomer with copper K_α line(λ = 1.54178 Å) as the incident beam. A gobel mirror was employed as monochromator. The sample powder was loaded to a glass holder and leveled with a glass slide before mounting it on the sample chamber. The specimens were scanned between 3 and 60^o. The scan step-width and rate were set to $0.01^o$and 0.01^o/s. Thermogravimetric analysis(TGA) was performed using a NETZSCH TG209 F3 and the sample is heated at a rate of 10^oC under N_2 gas environment. Elemental analysis was obtained from a ThermoFinnigan Instruments Flash EA1112 microelemental analyzer. The particle size and morphology was determined by a Hitachi S4800 scanning electron microscope (SEM). PL spectra were taken on Edinburgh Instruments F900. The excitation and the emission slit width were 1.0 and 1.0 nm, respectively, and scan step is 0.5 nm. The luminescence lifetime is excited by a □F900 lamp, the excitation and emission slit is 2.0 and 2.0 nm, respectively. The time range is 4~10 ms, peak count 2000 and the channel is 2000.

Table S1 Morphology simulation of an ideal crystal morphology of **NMOF 1**.

Predicated forms(multiplicity)	Total area (%)	Dhkl (Å)
{111}(8)	60.61	7.87
{004}(2)	17.80	6.86
{022}(4)	21.59	6.73

Table S2 Fluorescence lifetime of origin ethanol solution of **NMOF 1** hexagonal nanoplates and this solution with the different concentration of DPA (excited: 279 nm; monitored: 614 nm).

DPA (ppm)	τ_1 (μs)	τ_2 (μs)
0	100.10	387.09
0.2	122.20	395.89
0.4	167.75	431.87
0.8	256.37	618.15
1.2	320.70	1161.29
1.6	314.51	1450.76
2.0	344.07	1803.38

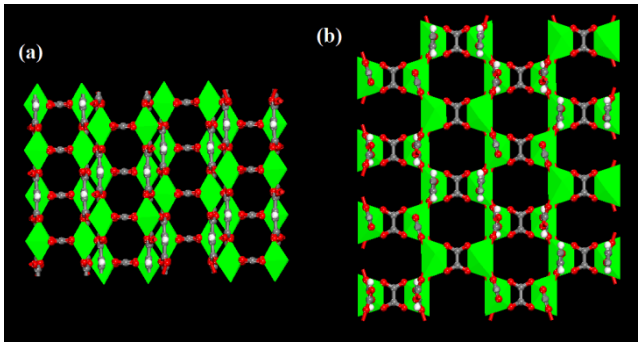

Figure S1 X-ray single crystal structure of **MOF 1** exhibiting two types of micropores of about (a) 3.8 × 3.8 Å along *b* axis and (b) 4.0 × 5.0 Å along *a* axis, respectively.

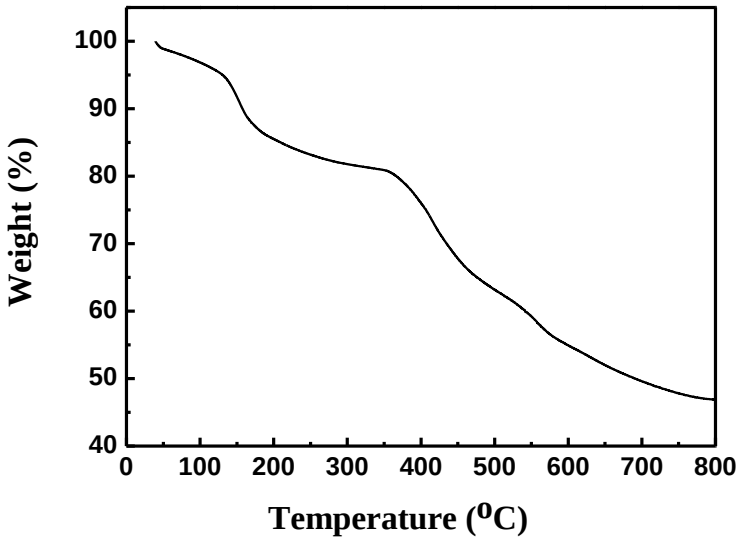

Figure S2. The TGA curve of **NMOF 1**.

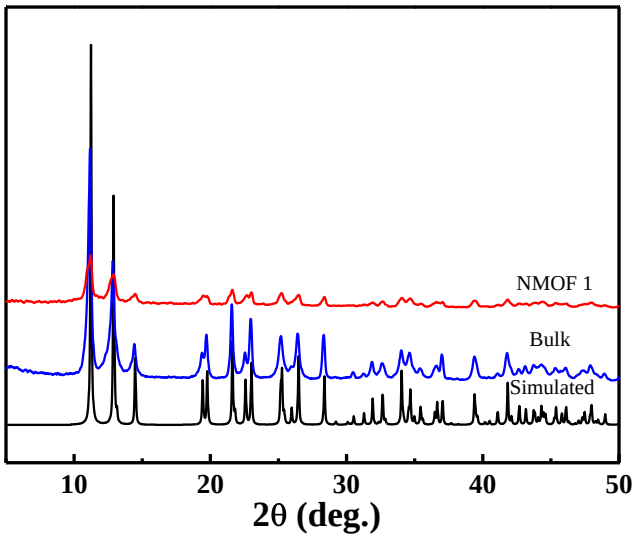

Figure S3. Powder X-ray diffraction patterns of the as-synthesized **NMOF 1** hexagonal nanoplates, bulk **MOF 1** and the one simulated from the X-ray single structure of **MOF 1**.

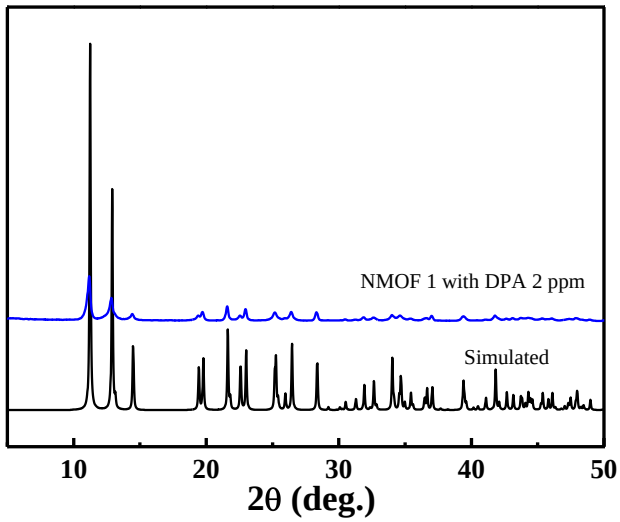

Figure S4. Powder X-ray diffraction patterns of the **NMOF 1** hexagonal nanoplates with the addition of 2 ppm DPA and the simulated one of bulk **MOF 1**.

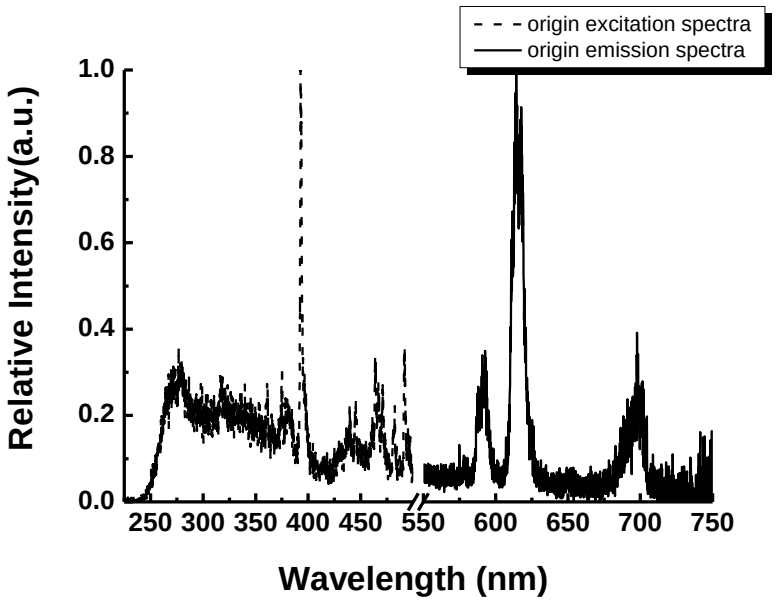

Figure S5. The excitation (dotted) and PL spectra (solid) of the origin ethanol solution of **NMOF 1** hexagonal nanoplates, monitored and excited at 616nm and 276nm, respectively.

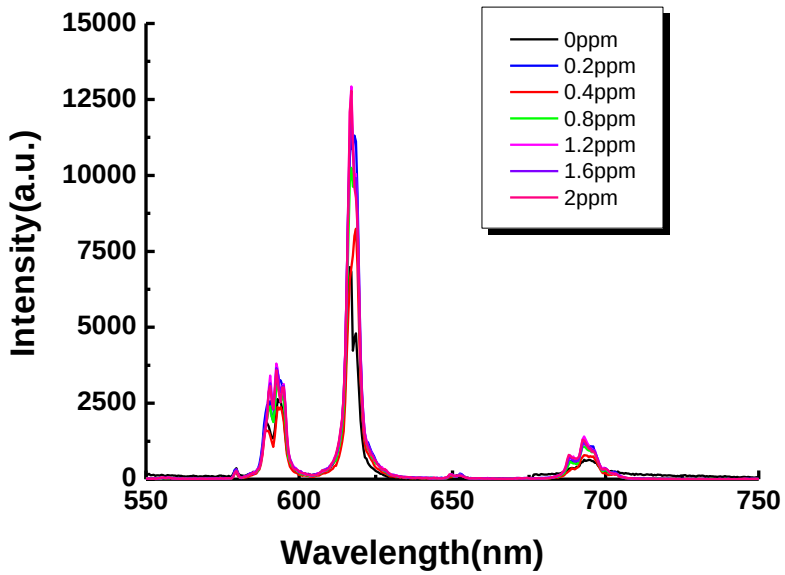

Figure S6. PL spectra of bulk **MOF 1** with the addition of different concentrations of DPA.

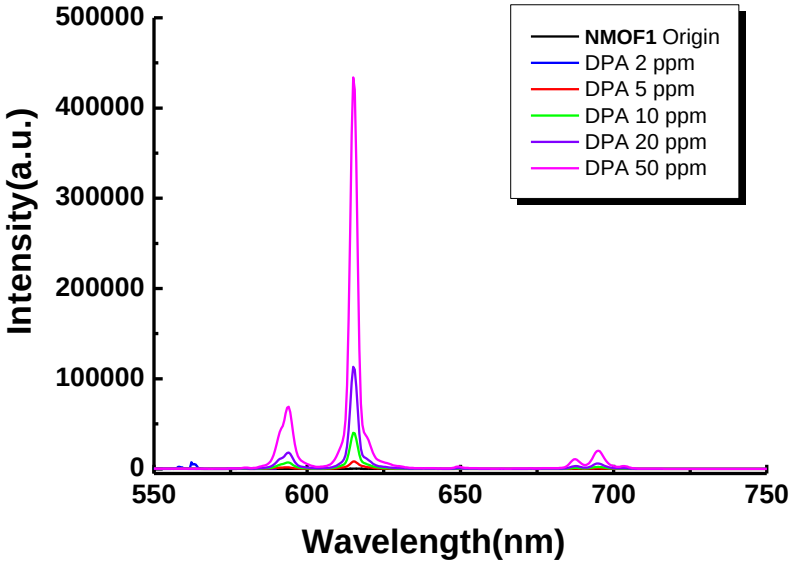

Figure S7. PL spectra of the ethanol solution of **NMOF 1** hexagonal nanoplates with the addition of different concentrations of DPA.

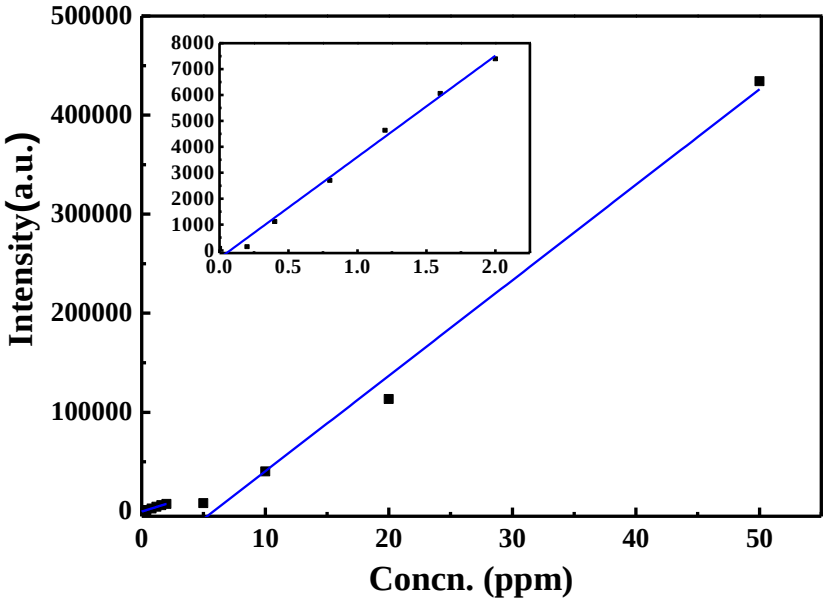

Figure S8. Dependence of $^5D_0$-$^7F_2$ luminescence intensity of **NMOF 1** on the low concentration and high concentration of DPA (insert: dependence of the luminescence intensity on low the DPA concentration).

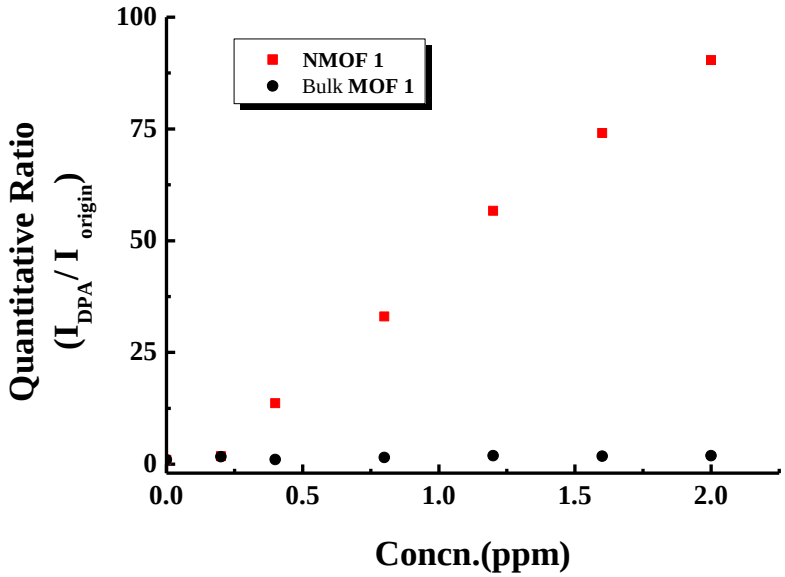

Figure S9. Quantitative ratio of fluorescent intensity of $^5D_0$-$^7F_2$ with the addition of different concentrations of DPA to the intensity of origin sample (red and black is **NMOF 1** and bulk **MOF 1**, respectively).

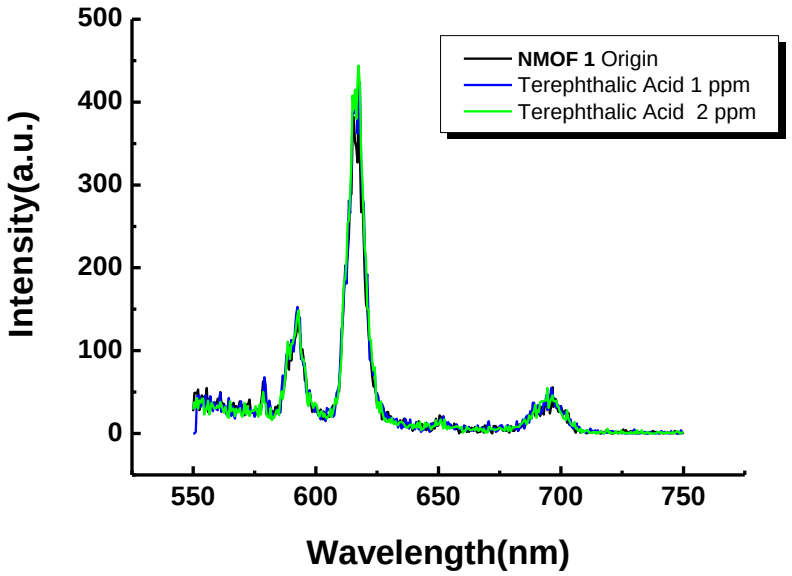

Figure S10. The PL spectra of the ethanol solution of **NMOF 1** hexagonal nanoplates with the addition of different concentrations of terephthalic acid, excited at 276 nm.

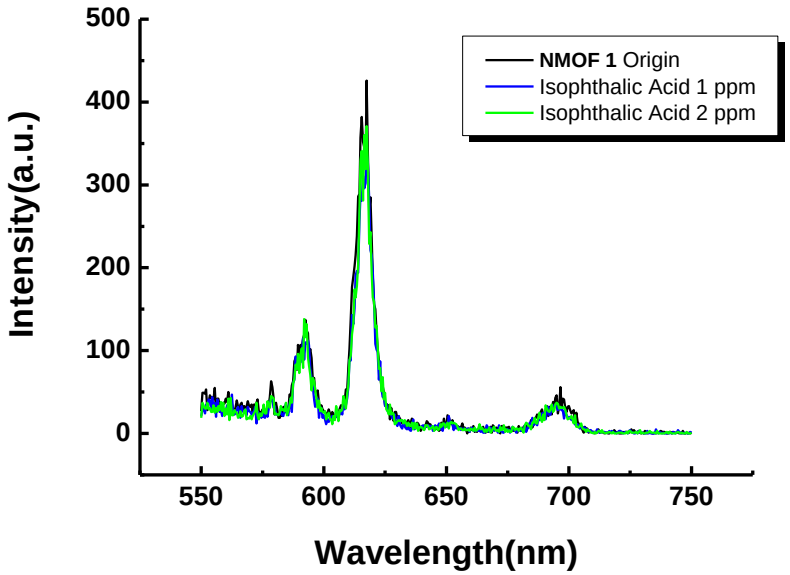

Figure S11. The PL spectra of the ethanol solution of **NMOF 1** hexagonal nanoplates with the addition of different concentrations of isophthalic acid, excited at 276 nm.

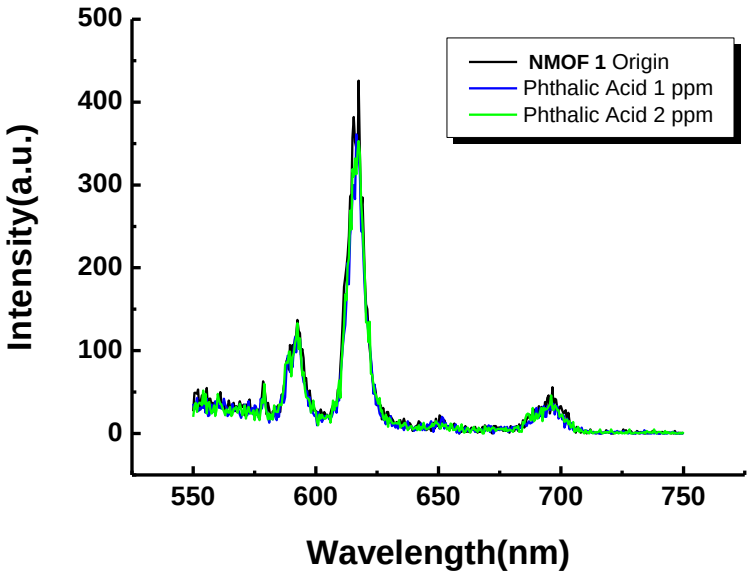

Figure S12. The PL spectra of the ethanol solution of **NMOF 1** hexagonal nanoplates with the addition of different concentrations of phthalic acid, excited at 276 nm.

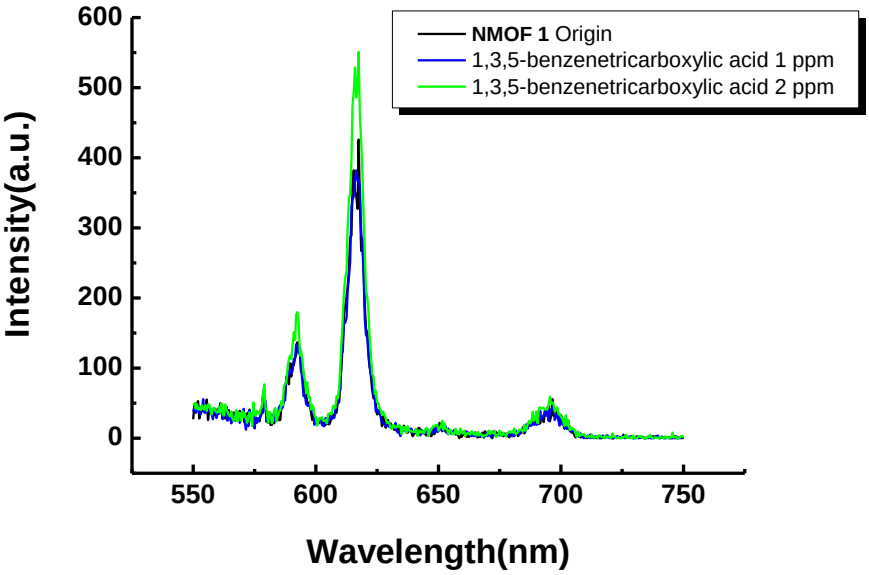

Figure S13. The PL spectra of the ethanol solution of **NMOF 1** hexagonal nanoplates with the addition of different concentrations of 1,3,5-benzenetricarboxylic acid, excited at 276 nm.

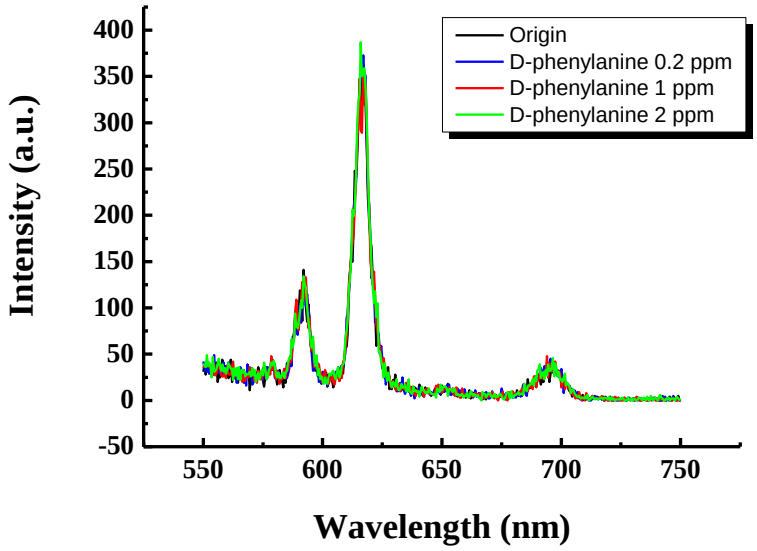

Figure S14. The PL spectra of the ethanol solution of **NMOF 1** hexagonal nanoplates with the addition of different concentration of D-phenylanine, excited at 276 nm.

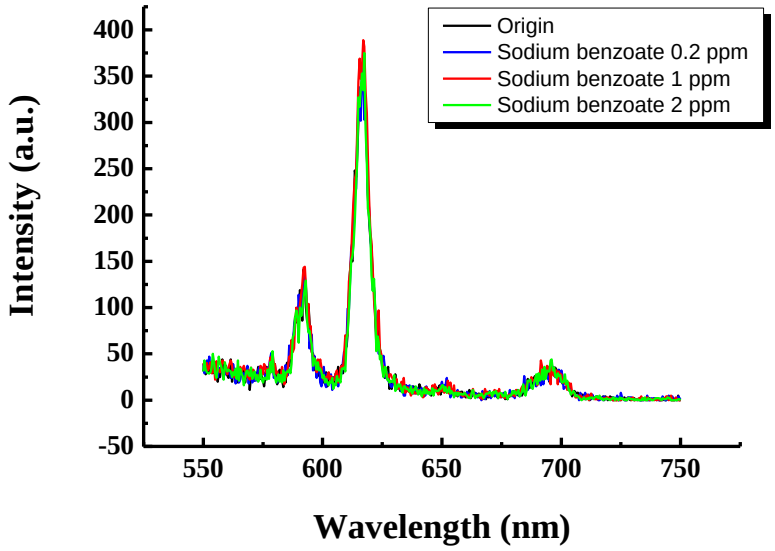

Figure S15. The PL spectra of the ethanol solution of **NMOF 1** hexagonal nanoplates with the addition of different concentration of sodium benzoate, excited at 276 nm.

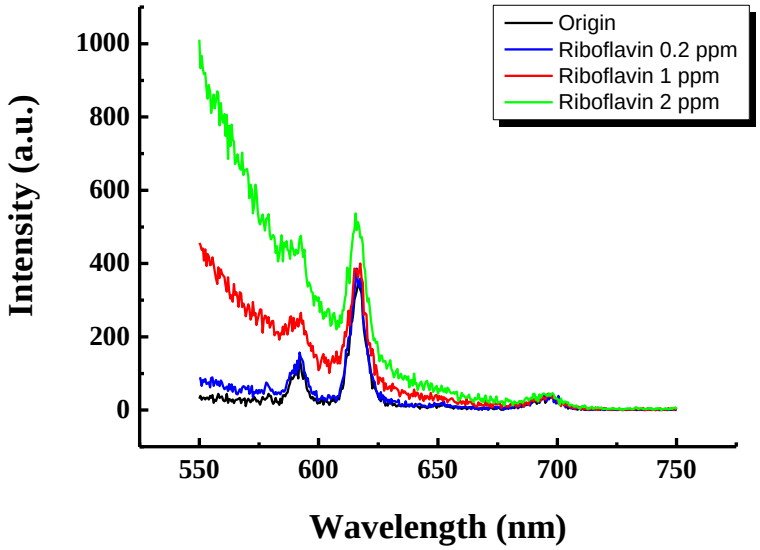

Figure S16. The PL spectra of the ethanol solution of **NMOF 1** hexagonal nanoplates with the addition of different concentration of riboflavin, excited at 276 nm.

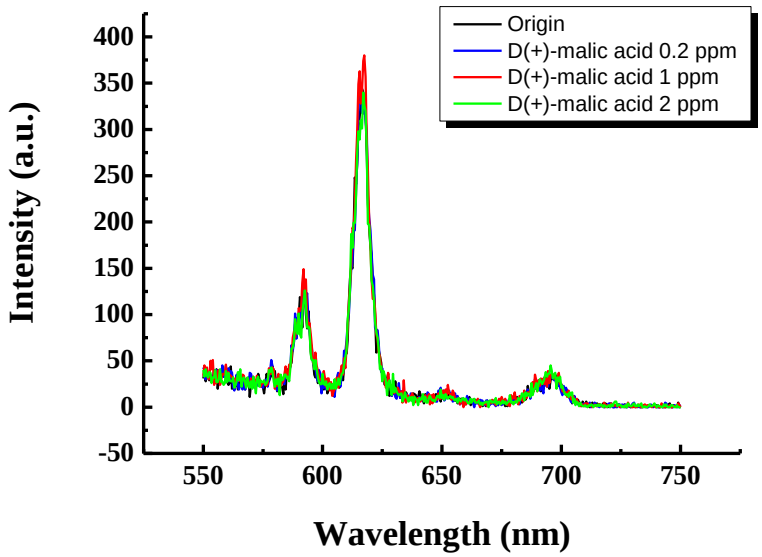

Figure S17. The PL spectra of the ethanol solution of **NMOF 1** hexagonal nanoplates with the addition of different concentration of D(+)-malic acid, excited at 276 nm.

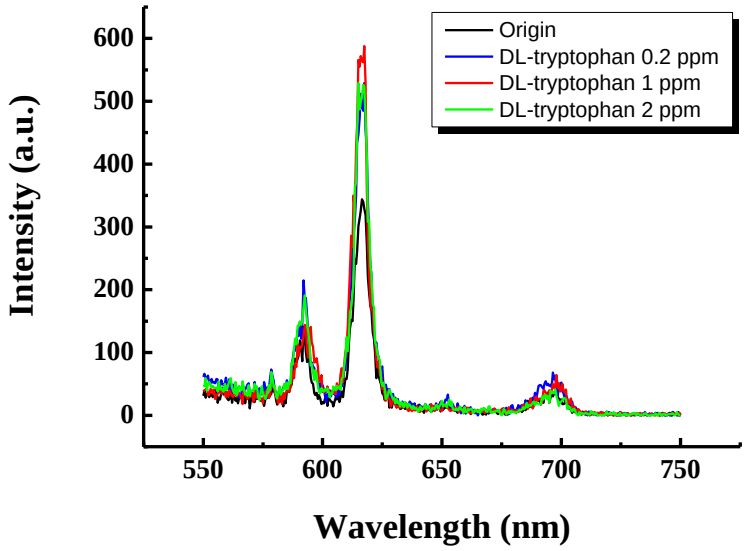

Figure S18. The PL spectra of the ethanol solution of **NMOF 1** hexagonal nanoplates with the addition of different concentration of DL-tryprophan, excited at 276 nm.

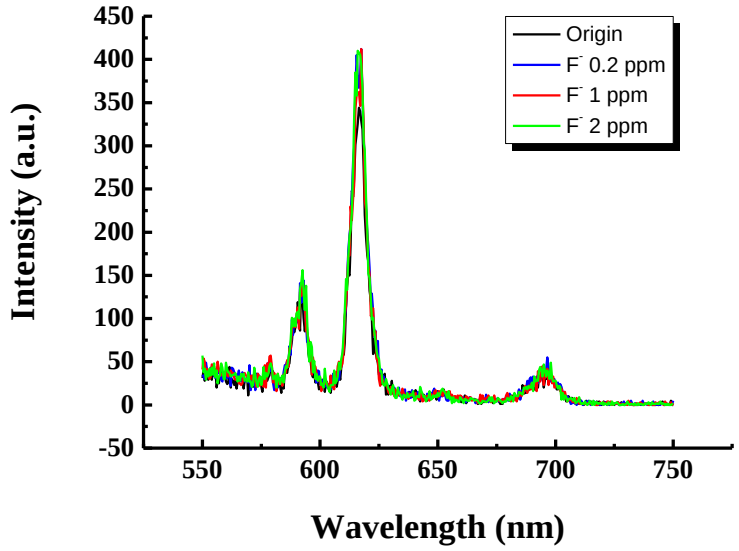

Figure S19. The PL spectra of the ethanol solution of **NMOF 1** hexagonal nanoplates with the addition of different concentration of F^-, excited at 276 nm.

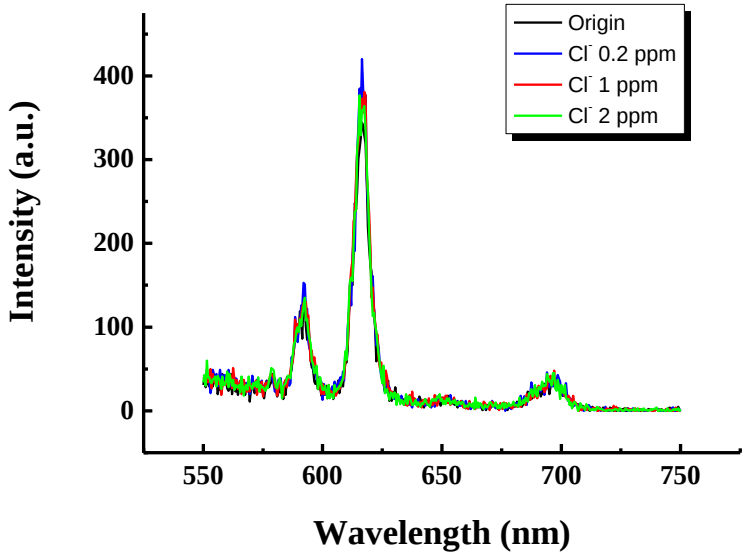

Figure S20. The PL spectra of the ethanol solution of **NMOF 1** hexagonal nanoplates with the addition of different concentration of Cl^-, excited at 276 nm.

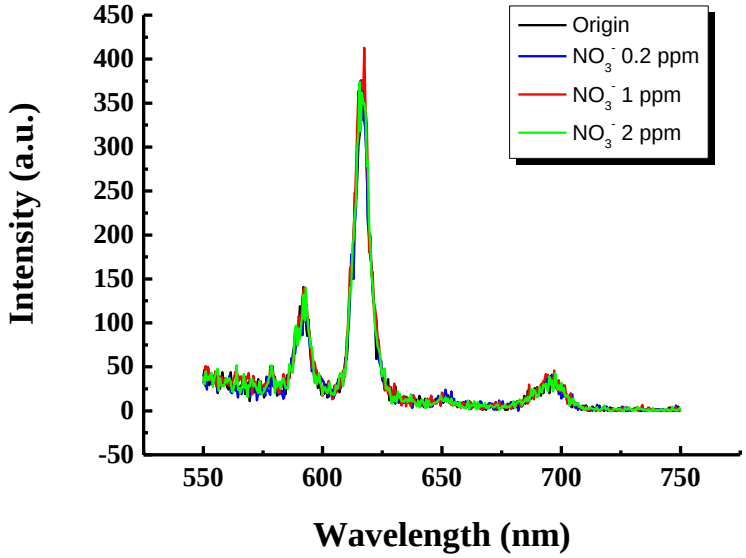

Figure S21. The PL spectra of the ethanol solution of **NMOF 1** hexagonal nanoplates with the addition of different concentration of NO_3^-, excited at 276 nm.

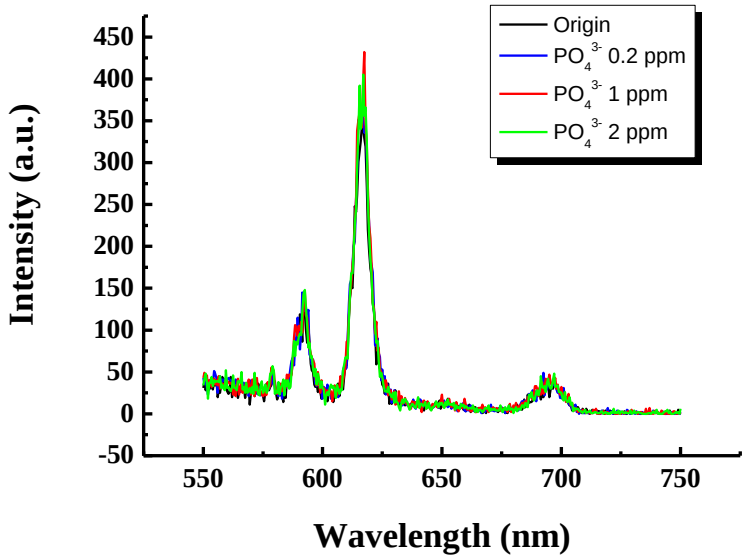

Figure S22. The PL spectra of the ethanol solution of **NMOF 1** hexagonal nanoplates with the addition of different concentration of PO_4^{3-}, excited at 276 nm.

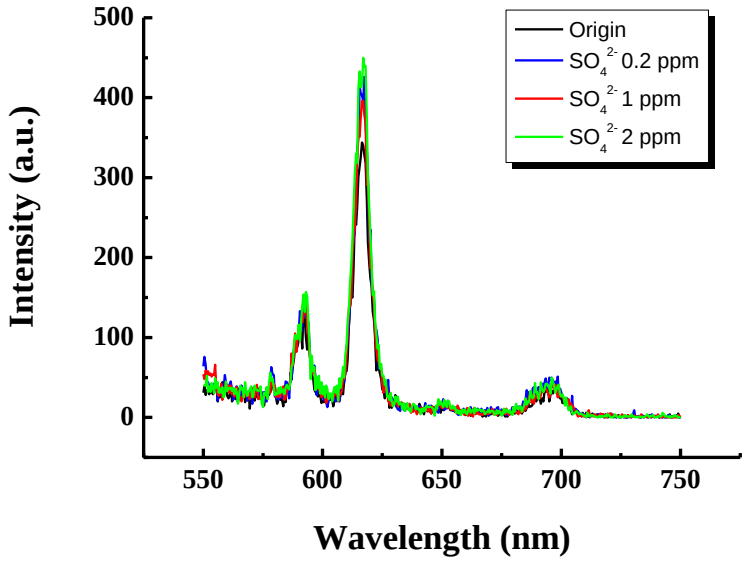

Figure S23. The PL spectra of the ethanol solution of **NMOF 1** hexagonal nanoplates with the addition of different concentration of SO_4^{2-}, excited at 276 nm.

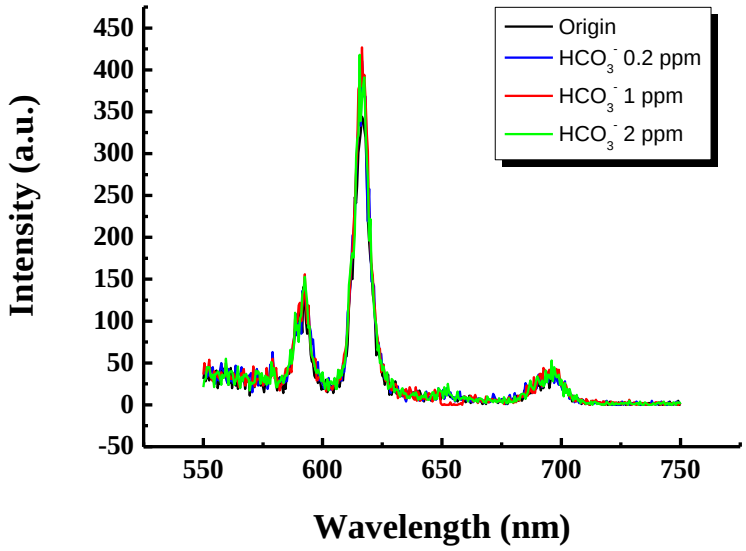

Figure S24. The PL spectra of the ethanol solution of **NMOF 1** hexagonal nanoplates with the addition of different concentration of HCO_3^-, excited at 276 nm.

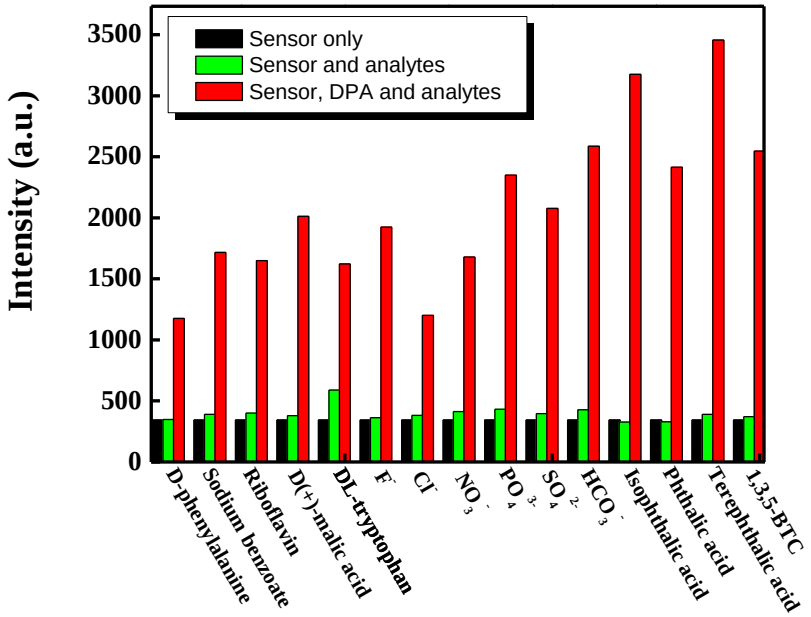

Figure S25. The fluorescence response of the ethanol solution of **NMOF 1** hexagonal nanoplates to 1.0 ppm DPA with the existence of 1.0 ppm another analyte.

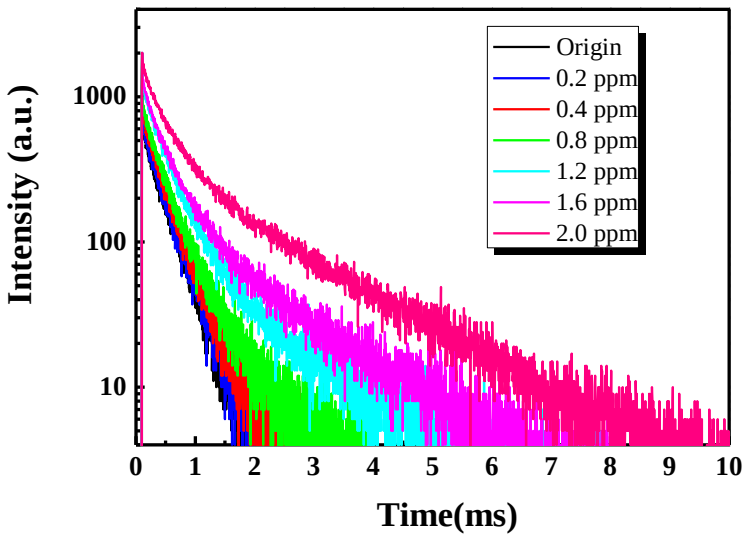

Figure S26. PL decay curves of **NMOF 1** in ethanol solution with the addition of different concentration DPA (excited: 279nm; monitored: 614 nm)